

Rare decays of the B_s – meson into four charged leptons in the framework of the Standard Model

A. V. Danilina^{1,2}, N. V. Nikitin^{2,3,4,‡}

¹Skobeltsyn Institute of Nuclear Physics, Moscow, Russia

²NRC "Kurchatov Institute" – ITEP, Moscow, Russia

³Lomonosov Moscow State University, Physics Faculty, Moscow, Russia

⁴The Moscow Institute of Physics and Technology, Dolgoprudny, Moscow Region, Russia

E-mail: anna.danilina@cern.ch, Nikolai.Nikitine@cern.ch

Abstract. In the framework of the Standard Model we present new theoretical predictions for the branching ratios, double and single differential distributions and forward – backward leptonic asymmetries for the $\bar{B}_s \rightarrow \mu^+\mu^-e^+e^-$ decay. In our consideration we take into account the $\phi(1020)$ – resonance contribution; the main contributions of four charmonium resonances : $\psi(3770)$, $\psi(4040)$, $\psi(4160)$ and $\psi(4415)$; $u\bar{u}$ – resonant contribution from $\rho(770)$ and $\omega(782)$; “tails” contributions from J/ψ and $\psi(2S)$ resonances; non – resonant contribution of the $b\bar{b}$ - pairs, bremsstrahlung and the contribution of the weak annihilation. We provide the prediction for the branching ratio of $\bar{B}_s \rightarrow \mu^+\mu^-e^+e^-$ decay with and without the $\phi(1020)$ – resonance contribution. We use the model of vector meson dominance (VMD) for calculation of resonances contributions and take into account all substantive terms in $\bar{B}_s \rightarrow \mu^+\mu^-e^+e^-$ amplitude that was not considered in the previously papers.

1. Introduction

The search for some deviations from the Standard Model (SM) predictions is the great challenge of high energy physics at the current moment. However, many experimental results are unclear and not explained in the SM. For example, an indication of the existence of dark matter in astrophysical experiments was well established [1]. At the present days it is the most powerful argument for the existence of new physics. There are a number of experimental indications of deviations from the SM predictions, such as violation of lepton universality in rare semileptonic B – decays; data on the anomalous magnetic moment of the muon, diverging from the SM predictions [2]; hints of a discrepancy between the experimental and predicted value of the partial widths for the $B_s \rightarrow \mu^+\mu^-$ decays [3, 4, 5, 6].

‡ Present address: Federal State Budget Educational Institution of Higher Education M.V.Lomonosov Moscow State University, Skobeltsyn Institute of Nuclear Physics (SINP MSU), 1(2), Leninskie gory, GSP-1, Moscow 119991, Russian Federation

It shows the great importance of the searching for statistically significant effects beyond the Standard Model (BSM) physics at modern and future accelerators, where, in contrast to astrophysical observations, the experiment is completely controlled and the systematic uncertainties are under the supervision.

In recent years, experimental data on weak decays of b – and c – quarks have gained importance in the study of BSM effects. Recent anomalies found in weak B – meson decays may be crucial [7]. There have been suggestions that a breakthrough in high energy physics can occur precisely from the analysis of weak decays of b – and c – quarks. In the next two years, for the implementation of this idea, a large amount of new data in heavy flavour physics is expected, primarily from the BELLE – II (KEK) and LHCb (LHC, CERN) experiments [8]. It will enable to advance in the study of very rare four – leptonic decays of B – mesons. These decays are suppressed in the SM, which makes them effective tools for searching for the effects of new physics. In that perspective, it is necessary to obtain reliable theoretical predictions for such extremely B – mesons decays and to understand which decays characteristics are the best for the looking for the manifestation of BSM effects.

The rare four – leptonic decays of B – mesons in SM can be divided into two types. The decays of the first type include a large number of electromagnetic and weak processes at the tree level realizing the final lepton state. A typical example of such decays are the decay $B^- \rightarrow \mu^+ \mu^- \mu^+ \bar{\nu}_\mu$ and similar decays of the charged B mesons. Decays of the second type are forbidden at the tree level and occur in higher orders of perturbation theory due to loop diagrams of the “penguin” and/or “box” type. The contribution of such processes can be described using Flavor Changing Neutral Currents (FCNC). In SM they are due to loop quantum diagrams, where the contribution of new virtual particles can be noticeable and measurable. An example of the second decays type is the processes $\bar{B}_{d,s} \rightarrow \mu^+ \mu^- e^+ e^-$ and $\bar{B}_{d,s} \rightarrow \mu^+ \mu^- \mu^+ \mu^-$. The first and second types of processes are being studied at the LHC and are planned to be studied at the Belle II facility. Currently, only upper limits are found for the partial widths of four – leptonic decays B_d and B_s [9], [10], [16]. Thus, a theoretical study of the rare leptonic decays of neutral $B_{d,s}^0$ – mesons is one of great problem for further investigations on the LHC and other experiments. At the moment, for these decays there is only a prediction given in the [12], which does not take into account the many resonant contributions, and an rough estimation from [13].

In this paper we present the detailed calculation of the branching ratio of $\bar{B}_s \rightarrow \mu^+ \mu^- e^+ e^-$ and differential characteristics, taking into account contributions of $\phi(1020)$ – resonance, the main contributions of charmonium resonances, non – resonance contribution of the $b\bar{b}$ – pairs, leading contribution of weak annihilation and bremsstrahlung.

2. Effective Hamiltonian

The FCNC $b \rightarrow q$ (where $q = \{d, s\}$) effective Hamiltonian have the form of the Wilson expansion [14]:

$$\mathcal{H}_{eff}^{b \rightarrow q}(x, \mu) = \frac{G_F}{\sqrt{2}} V_{tq}^* V_{tb} \sum_i C_i(\mu) O_i^{b \rightarrow q}(x),$$

where $\mu \approx m_b$ is the scale parameter which separates short and long distance contributions of the strong interactions, G_F is the Fermi constant, V_{tq} and V_{tb} are the matrix elements of the Cabibbo-Kobayashi-Maskawa (CKM) matrix. The light degrees of freedom of the SM, such as u, d, s, c , and b - quarks, leptons, photons and gluons are contained in the basis operators $O_i^{b \rightarrow q}(x, \mu)$. The heavy degrees of freedom, W, Z , and t - quark, are introduced into the Wilson coefficients $C_i(\mu)$. The sign of the Wilson coefficients is determined by the condition $C_2(M_W) = -1$.

To calculate the amplitude of the decay $\bar{B}_s \rightarrow \mu^+ \mu^- e^+ e^-$ the Hamiltonian for the FCNC transition $b \rightarrow s \ell^+ \ell^-$ is used:

$$\begin{aligned} \mathcal{H}_{eff}^{b \rightarrow s \ell^+ \ell^-}(x, \mu) = & \frac{G_F}{\sqrt{2}} \frac{\alpha_{em}}{2\pi} V_{tb} V_{ts}^* \left[-2 \frac{C_{7\gamma}(\mu)}{q^2} \left\{ m_b (\bar{s} i \sigma_{\mu\nu} (1 + \gamma_5) q^\nu b) \right. \right. \\ & + m_s (\bar{s} i \sigma_{\mu\nu} (1 - \gamma_5) q^\nu b) \left. \right\} \cdot (\bar{\ell} \gamma^\mu \ell) \\ & + C_{9V}^{eff}(\mu, q^2) (\bar{s} O_\mu b) \cdot (\bar{\ell} \gamma^\mu \ell) + C_{10A}(\mu) (\bar{s} O_\mu b) \cdot (\bar{\ell} \gamma^\mu \gamma_5 \ell) \left. \right], \end{aligned} \quad (1)$$

where $O_\mu = \gamma_\mu (I - \gamma_5)$ and q^ν is the four - momentum of $\ell^+ \ell^-$ - pair, the matrix γ^5 is defined as $\gamma^5 = i\gamma^0 \gamma^1 \gamma^2 \gamma^3$, $\varepsilon^{0123} = -1$ and $\sigma_{\mu\nu} = \frac{i}{2} [\gamma_\mu, \gamma_\nu]$.

In accordance with definition (Eq.1) the Hamiltonian of the electromagnetic interaction has the form:

$$\mathcal{H}_{em}(x) = -e \sum_f Q_f (\bar{f}(x) \gamma^\mu f(x)) A_\mu(x) = -j_{em}^\mu A_\mu(x), \quad (2)$$

where the charge $e = |e| > 0$ is normalized by $e^2 = 4\pi\alpha_{em}$; $\alpha_{em} \approx 1/137$ is the fine structure constant; Q_f is the charge of the fermion of flavor f in units of the e , $f(x)$ is the fermionic field of flavor f and $A_\mu(x)$ is the four-potential of the electromagnetic field.

The Hamiltonian for the weak annihilation has the form

$$\mathcal{H}_{eff}^{\bar{B}_s - Q \bar{Q}}(x) = -\frac{G_F}{\sqrt{2}} V_{Qb} V_{Qq}^* a_1(\mu) (\bar{q} O^\mu b) (\bar{Q} O_\mu Q), \quad (3)$$

where $Q = \{u, c\}$ and $a_1(\mu = 5 \text{ GeV}) \approx -0.13$.

3. Main contributions to the $\bar{B}_s \rightarrow \mu^+ \mu^- e^+ e^-$ decay

There are six main types of contributions are required for the description of the decays $\bar{B}_s \rightarrow \mu^+(k_1) \mu^-(k_2) e^+(k_3) e^-(k_4)$. The first type arises in the situation when

a virtual photon is emitted from s – quark (see Fig. 1). The second type is related to bremsstrahlung, when a virtual photon is emitted by the lepton in the final state (see Fig. 3). The third and fourth types reflect the contributions from $u\bar{u}$ and $c\bar{c}$. The fifth type corresponding to the $b\bar{b}$ – pair’s contribution shown on the Fig. 2. And the last one tied to the weak annihilation processes (see Fig. 4). The momenta $q = k_1 + k_2$ and $k = k_3 + k_4$ (see Appendix A1).

Using the Hamiltonians (Eq.1,2 and 3) we can find, that the amplitude for a process of virtual photon emission by s – quark as well as the $u\bar{u}$, $c\bar{c}$ and $b\bar{b}$ – pairs contributions can be presented as

$$\begin{aligned} \mathcal{M}_{fi}^{(1234)} = & i \sqrt{2} G_F \alpha_{em}^2 V_{tb} V_{ts}^* M_1 \left[\right. \\ & \left[-\frac{a^{(VV)}}{M_1^2} \varepsilon_{\mu\alpha k q} - i b^{(VV)} g_{\mu\alpha} + 2i \frac{c^{(VV)}}{M_1^2} q_\alpha k_\mu \right] j^\mu(k_2, k_1) J^\alpha(k_4, k_3) + \\ & + \left[-\frac{a^{(VA)}}{M_1^2} \varepsilon_{\mu\alpha k q} - i b^{(VA)} g_{\mu\alpha} + 2i \frac{c^{(VA)}}{M_1^2} q_\alpha k_\mu + i \frac{g^{(VA)}}{M_1^2} k_\mu k_\alpha \right] j^\mu(k_2, k_1) J^{\alpha 5}(k_4, k_3) + \\ & + \left[-\frac{a^{(AV)}}{M_1^2} \varepsilon_{\mu\alpha k q} - i b^{(AV)} g_{\mu\alpha} + 2i \frac{c^{(AV)}}{M_1^2} q_\alpha k_\mu + i \frac{d^{(AV)}}{M_1^2} q_\mu k_\alpha \right] j^{\mu 5}(k_2, k_1) J^\alpha(k_4, k_3) + \\ & + \left[-\frac{a^{(AA)}}{M_1^2} \varepsilon_{\mu\alpha k q} - i b^{(AA)} g_{\mu\alpha} + 2i \frac{c^{(AA)}}{M_1^2} q_\alpha k_\mu + i \frac{d^{(AA)}}{M_1^2} q_\mu k_\alpha + i \frac{g^{(AA)}}{M_1^2} k_\mu k_\alpha \right] j^{\mu 5}(k_2, k_1) J^{\alpha 5}(k_4, k_3) \left. \right], \end{aligned} \quad (4)$$

where currents are defined as

$$\begin{aligned} j^\mu(k_2, k_1) &= \bar{\mu}(k_2) \gamma^\mu \mu(-k_1), \quad J^\alpha(k_4, k_3) = \bar{e}(k_4) \gamma^\alpha e(-k_3); \\ j^{\mu 5}(k_2, k_1) &= \bar{\mu}(k_2) \gamma^\mu \gamma^5 \mu(-k_1), \quad J^{\alpha 5}(k_4, k_3) = \bar{e}(k_4) \gamma^\alpha \gamma^5 e(-k_3). \end{aligned}$$

Dimensionless functions $a^{(IJ)} \equiv a^{(IJ)}(x_{12}, x_{34})$, $b^{(IJ)} \equiv b^{(IJ)}(x_{12}, x_{34})$, $c^{(IJ)} \equiv c^{(IJ)}(x_{12}, x_{34})$, $d^{(IJ)} \equiv d^{(IJ)}(x_{12}, x_{34})$ and $g^{(IJ)} \equiv g^{(IJ)}(x_{12}, x_{34})$, where $IJ = \{VV, VA, AV, AA\}$ are defined in Appendix B.

The contribution to the decay amplitude (Eq.4) from Fig.1 may be calculated using the Vector Meson Dominance model (VMD). Here we consider two cases: a virtual photon emission produces a $\mu^+\mu^-$ – pair (left diagram) and a virtual photon emission produce a e^+e^- – pair (right diagram). In both cases there is the intermediate vector $\phi(1020)$ – meson that we take into account in the framework of VMD (as reflected in $a^{(IJ)}$, $b^{(IJ)}$, $c^{(IJ)}$, $d^{(IJ)}$ and $g^{(IJ)}$ coefficients in Appendix B). As the further calculations will show, the $\phi(1020)$ – resonance gives a leading contribution to the amplitude of $\bar{B}_s \rightarrow \mu^+\mu^-e^+e^-$ decay.

Charmonium vector resonances and $\rho^0(770)$, $\omega(782)$ contributions are arised from the effective Hamiltonian for the transition $b \rightarrow s\ell^+\ell^-$ (Eq.1) and contained in coefficients $a^{(IJ)}$, $b^{(IJ)}$ and $c^{(IJ)}$. The resonant contributions from J/ψ , $\psi(2S)$..., $\rho^0(770)$ and $\omega(782)$ are contained in the coefficient $C_{9V}^{eff}(\mu, q^2)$. This coefficient consists of

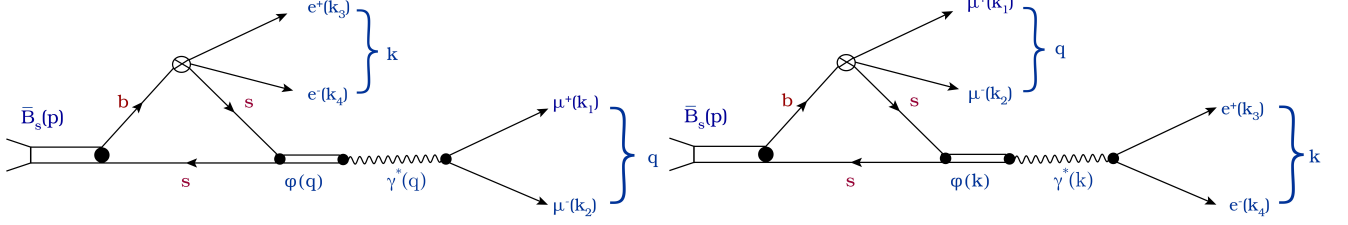


Figure 1. Emission diagram of a virtual photon by a s – quark of B_s meson.

the fixed part, depending on μ – scale, $c\bar{c}$ and $u\bar{u}$ quark loops contribution and vector resonances contribution.

The structure of the $C_{9V}^{eff}(\mu, q^2)$ may be presented as

$$C_{9V}^{eff}(\mu, q^2) = C_{9V}(\mu) + \Delta C_{9V}^{c\bar{c}+u\bar{u}}(\mu, s),$$

where $C_{9V}(\mu)$ is the Wilson coefficient ($C_{9V}(\mu = m_b) = -4.21$) and $\Delta C_{9V}^{c\bar{c}+u\bar{u}}(\mu, s)$ is non-perturbative correction, consisting of loop and resonant effects.

In the factorization approximation the structure of the $\Delta C_{9V}^{c\bar{c}}(\mu, s)$ is given in Ref. [17].

In according to the experimental procedure of the J/ψ and $\psi(2S)$ contributions exclusion [9, 10, 16] in the theoretical calculation of the differential characteristics and branching ratio of $\bar{B}_s \rightarrow \mu^+ \mu^- e^+ e^-$ decay we leave only tails from J/ψ and $\psi(2S)$ resonances. The higher vector charmonium contributions are not cut, since they don't overlap less significant contributions.

The next contribution to the (Eq. 4) amplitude is the non-resonant contribution from $b\bar{b}$ – pairs (Fig.2).

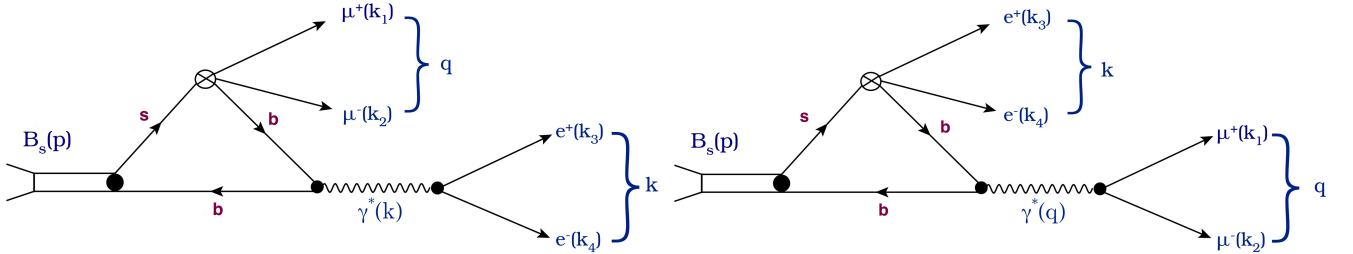


Figure 2. Emission diagrams of a virtual photon by a b – quark of B_s meson

Using the numerical calculation $F_i(0, 0)$ and M_{R_i} from Ref. [18], it is possible to find the following parameterization for the non-resonant form factor:

$$F_i(q_1^2, q_2^2) = \frac{F_i(q_1^2 = 0, q_2^2 = 0)}{\left(1 - \frac{q_1^2}{M_{R_i}^2}\right) \left(1 - \frac{q_2^2}{M_{Y(1S)}^2}\right)},$$

where $i = \{V, A, TV, TA\}$.

As $M_{B_s^*} > M_1$, this pole lies outside of the kinematically allowed range of the decay $\bar{B}_s \rightarrow \mu^+ \mu^- e^+ e^-$. The existence of this pole is taken into account when choosing the pole parameterisation of the form factors.

The next set of diagrams is related to bremsstrahlung, when a virtual photon is emitted by one of lepton in the final state (see Fig. 3). There are four types of diagrams, for the photon emission by each lepton in the final state accordingly.

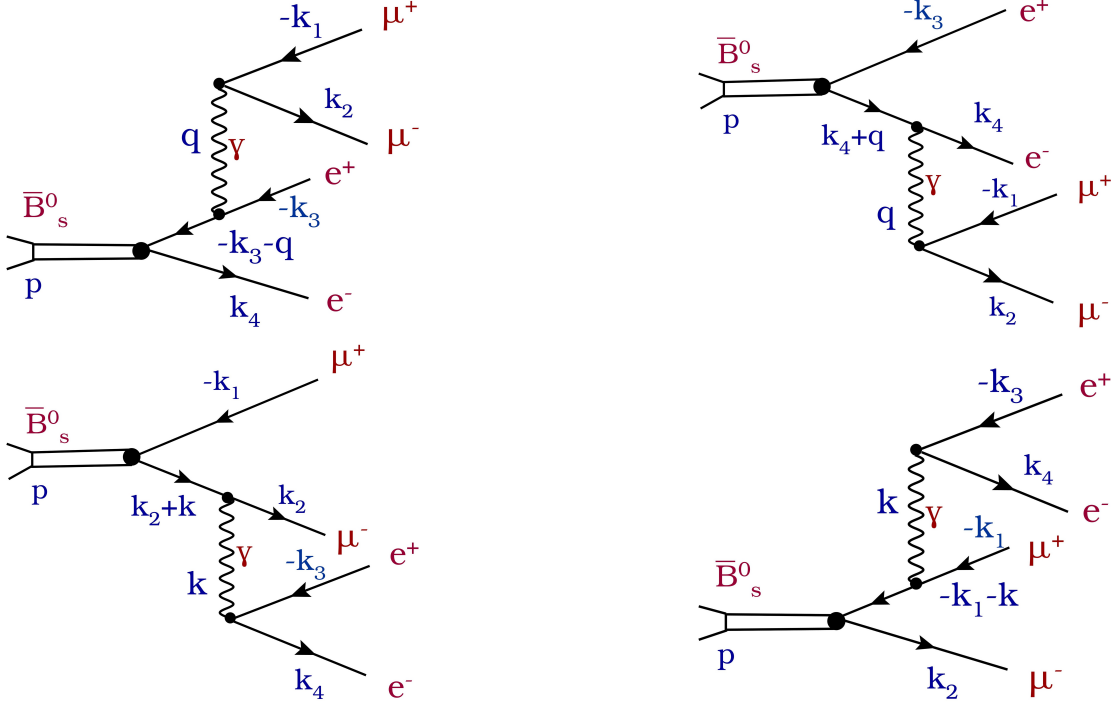


Figure 3. Emission diagram of a virtual photon by leptons in the final state.

The amplitude for the $\mu^+\mu^-$ pair emitted by electron and positron in the final state is:

$$\begin{aligned} \mathcal{M}_{fi}^{(\mu)} = & i\sqrt{2} G_F \alpha_{em}^2 V_{tb} V_{ts}^* \left(\bar{\mu}(k_2) \gamma^\mu \mu(-k_1) \right) \left[\right. \\ & i d^{(VP)}(x_{12}, x_{123}, x_{124}) k_\mu \left(\bar{e}(k_4) \gamma^5 e(-k_3) \right) + \\ & \left. + f^{(VT)}(x_{12}, x_{123}, x_{124}) \varepsilon_{\mu\nu\alpha\beta} p^\nu \left(\bar{e}(k_4) \gamma^\alpha \gamma^\beta e(-k_3) \right) \right]. \end{aligned} \quad (5)$$

The similar expression can be obtained for the e^+e^- pair emitted by muons in the final state. But for short, we do not write it here. For the calculation of the pole structure in bremsstrahlung non-zero lepton masses should be taken into account. It is done in the (Eq.5) and in the expression for four-particle phase space in the Appendix A.

The last contribution that we consider is the weak annihilation processes. These ones arise from lowest order diagrams describing contribution of $c\bar{c}$ and $u\bar{u}$ after integrating out the W bosons degrees of freedom. We taken into consideration axial anomaly contribution gives the following amplitude structure:

$$\begin{aligned} \mathcal{M}_{fi}^{(WA)} = & i \frac{32\sqrt{2}}{3\pi} \frac{G_F}{M_1^3} \alpha_{em}^2 (V_{ub} V_{us}^* + V_{cb} V_{cs}^*) a_1(\mu) \hat{f}_{B_s} \\ & \frac{1}{x_{12} x_{34}} \varepsilon_{\mu\alpha k q} \left(\bar{\mu}(k_2) \gamma^\mu \mu(-k_1) \right) \left(\bar{e}(k_4) \gamma^\alpha e(-k_3) \right), \end{aligned}$$

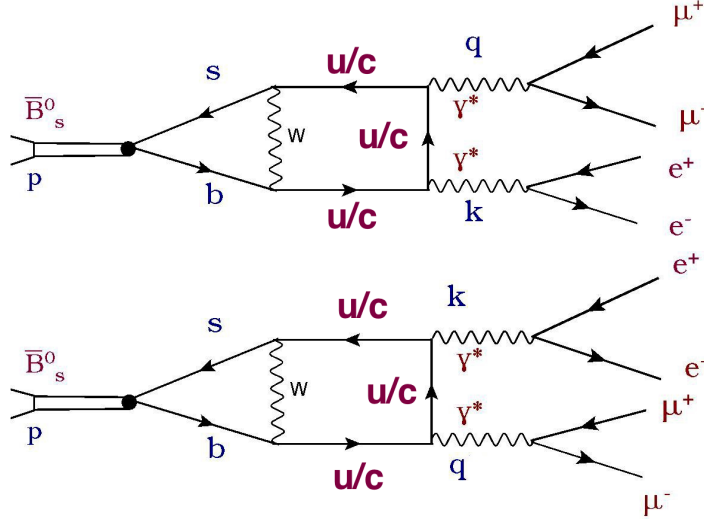


Figure 4. The diagrams for the weak annihilation processes.

where $\hat{f}_{B_s} = \frac{f_{B_s}}{M_1}$. Here we neglect $(m_c/M_1)^2$ and $(m_u/M_1)^2$ corrections.

The weak annihilation contribution is enhanced at small four-momenta, but even here it is suppressed by a power of a heavy quark mass compared to the contributions discussed in the previous paragraphs.

4. The branching ratio calculation

The extremely rare $B_{d,s}$ – decays provide the vigorous studies in the direction on the searches of physics beyond the Standard Model. From this point of view, detailed investigation of $\bar{B}_s \rightarrow \mu^+ \mu^- e^+ e^-$ decays is very promising. It demands the correct simulation of this decays. For that reason we produce the Monte Carlo model for the EvtGen package [15]. This model provides correct simulation for $\bar{B}_s \rightarrow \mu^+ \mu^- e^+ e^-$ decay and include all theoretical contributions which described in the Sec. 3. The tools of the EvtGen package allows to calculate the numerical value of the branching ratio of the $\bar{B}_s \rightarrow \mu^+ \mu^- e^+ e^-$ decay.

The total amplitude of the decay $\bar{B}_s \rightarrow \mu^+ \mu^- e^+ e^-$ can be presented in the form:

$$\mathcal{M}^{(tot)} = \mathcal{M}_{fi}^{(BS \ e+\mu)} + \mathcal{M}_{fi}^{(\phi)} + \mathcal{M}_{fi}^{(b\bar{b})} + \mathcal{M}_{fi}^{(c\bar{c}+u\bar{u})} + \mathcal{M}_{fi}^{(WA)} = \sqrt{2} G_F \alpha_{em}^2 V_{tb} V_{ts}^* \sum_L L j_1 j_2,$$

where j_1 and j_2 are lepton currents, L are the Lorentz structures contributed to this matrix element.

The differential branching ratio of the decay $\bar{B}_s \rightarrow \mu^+ \mu^- e^+ e^-$ has the form

$$\begin{aligned} d\text{Br}(\bar{B}_s \rightarrow \mu^+ \mu^- e^+ e^-) &= \tau_{B_s} \frac{\sum_{s_1, s_2, s_3, s_4} |\mathcal{M}_{fi}^{(tot)}|^2}{2M_1} d\Phi_4 = \\ &= \frac{G_F^2 \alpha_{em}^4 |V_{tb} V_{ts}^*|^2}{M_1} \tau_{B_s} \left| \sum_L L j_1 j_2 \right|^2 d\Phi_4 \end{aligned}$$

where τ_{B_s} is the lifetime of the B_s -meson, four-particle phase space $d\Phi_4$ is defined by (Eq.A.2). The summation is performed over the spins of the final leptons s_1, s_2, s_3 and s_4 . Full integration may be performed only numerically. By implementing built-in opportunity of the EvtGen package we realized the multidimensional integrator based on the effective geometry Monte Carlo algorithm. Within this approach, the branching ratio of the $\bar{B}_s \rightarrow \mu^+ \mu^- e^+ e^-$ decay may calculate as

$$\text{Br}(\bar{B}_s \rightarrow \mu^+ \mu^- e^+ e^-) \approx \frac{\alpha_{em}^4 |V_{tb} V_{ts}^*|^2}{3 \cdot 2^{13} \cdot \pi^5} \tau_{B_s} G_F^2 M_1^5 \frac{N_0}{N_{tot}} |X|^2,$$

where N_{tot} is total and N_0 is accepted numbers of events produced by EvtGen. $|X|^2 \equiv \max \frac{|\sum_L L j_1 j_2|^2}{M_1^2}$ is the dimensionless maximum of the decay matrix element. In the last formula we used the massless approach of the phase space. In the framework of the EvtGen we have the four - particle phase space with non - zero leptonic masses. The approach of multidimensional integration in the EvtGen has been tested on the already known branching ratios of several decays, as well as on the various functions, including the singular. Numerical integration for the $\bar{B}_s \rightarrow \mu^+ \mu^- e^+ e^-$ decay gives:

$$\text{Br}(\bar{B}_s \rightarrow \mu^+ \mu^- e^+ e^-) \approx (61 \pm 12) * 10^{-10}.$$

Here the J/ψ and $\psi(2S)$ resonances contributions are excluded from the calculation of the $\text{Br}(\bar{B}_s \rightarrow \mu^+ \mu^- e^+ e^-)$ according to experimental procedure [9]. If we exclude J/ψ and $\psi(2S)$ contributions following the conditions $\sqrt{|M_1^2 x_{ij} - m^2(Res)|} < 100 \text{ MeV}$ and the $\phi(1020)$ contribution with the condition $\sqrt{|M_1^2 x_{ij} - m^2(\phi(1020))|} < 70 \text{ MeV}$ according to the [16], we get the second value for the $\text{Br}(\bar{B}_s \rightarrow \mu^+ \mu^- e^+ e^-)$ decay:

$$\text{Br}(\bar{B}_s \rightarrow \mu^+ \mu^- e^+ e^-) \approx (2.8 \pm 0.5) * 10^{-10}.$$

Based on the our numerical predictions of the $\text{Br}(\bar{B}_s \rightarrow \mu^+ \mu^- e^+ e^-)$ it is possible to use the following estimate for the branching ratio of $\bar{B}_s \rightarrow \mu^+ \mu^- \mu^+ \mu^-$ decay. If we exclude the $\phi(1020)$ resonances contribution, in accordance with [12] we get

$$\text{Br}(\bar{B}_s \rightarrow \mu^+ \mu^- e^+ e^-) : \text{Br}(\bar{B}_s \rightarrow \mu^+ \mu^- \mu^+ \mu^-) = 3 : 1.$$

We have

$$\text{Br}(\bar{B}_s \rightarrow \mu^+ \mu^- \mu^+ \mu^-) \sim 10^{-10}.$$

This estimation does not contradict to the experimental upper limit [16]:

$$\text{Br}_{Exp}(\bar{B}_s \rightarrow \mu^+ \mu^- \mu^+ \mu^-) \leq 8.6 * 10^{-10}$$

and is consistent with the estimation from [13].

5. Differential distributions

We study the set of differential characteristics for the $\bar{B}_s \rightarrow \mu^+\mu^-e^+e^-$ decay, that demonstrate the features of this rare four – leptonic decay. We take into account contributions of $\phi(1020)$, $\psi(3770)$, $\psi(4040)$, $\psi(4160)$, $\psi(4415)$, $\rho^0(770)$ and $\omega(782)$ resonances and “tails” from the J/ψ and $\psi(2S)$ resonances.

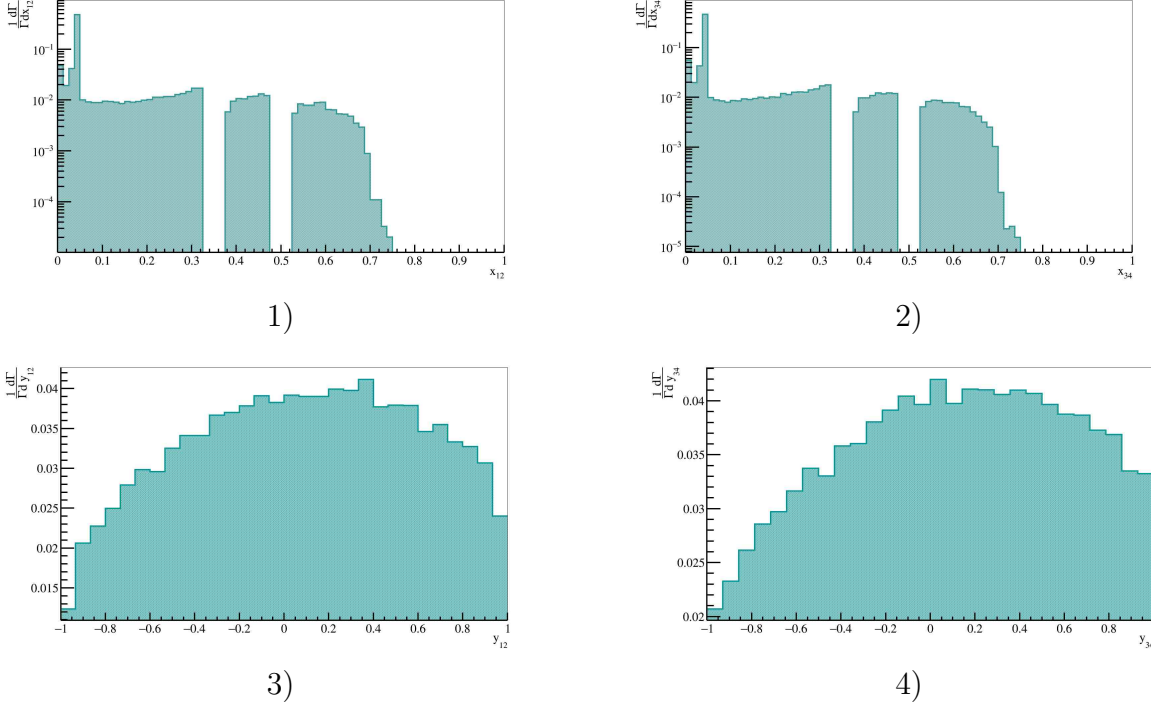


Figure 5. 1) x_{12} - distribution for the $\mu^+\mu^-$ - pair; 2) x_{34} - distribution for the e^+e^- - pair ; 3) $\cos(\theta_{12})$ - distribution; 4) $\cos(\theta_{34})$ - distribution.

We consider differential distributions for the decay $\bar{B}_s \rightarrow \mu^+\mu^-e^+e^-$. One-dimensional differential distribution by x_{12} and x_{34} are given in Fig. 5(1) and Fig. 5(2) respectively. Here we exclude J/ψ resonance region in accordance with conditions $\sqrt{|M_1^2x_{12} - m^2(J/\psi)|} < 100$ MeV. We have the same kinematical cut for the $\psi(2S)$ meson: $\sqrt{|M_1^2x_{12} - m^2(\psi(2S))|} < 100$ MeV. These restrictions selected according to experimental cuts [16]. The same cuts we use for the x_{34} . For the differential distributions the $\phi(1020)$ resonance is not excluded. In the Fig. 5(1) it is shown a photon pole for $x_{12} \rightarrow x_{12min} = (2m_\mu/M_1)^2 = 0.0016$ and a peak from the $\phi(1020)$ resonance for $x_{12} \rightarrow (M_\phi/M_1)^2 \approx 0.037$. Due to the fact that the $\phi(1020)$ meson contribution is very high, the contributions from other resonances near 1 GeV ($\rho^0(770)$ and $\omega(782)$ mesons) are not visible in Fig. 5(1). The distributions by x_{34} in Fig. 5(2) also reflect $\phi(1020)$ resonance contribution. It is generally symmetrical to the Fig. 5(1).

The distributions of the angular variables $y_{12} = \cos\theta_{12}$ and $y_{34} = \cos\theta_{34}$ are presented in Fig. 5(3) and Fig. 5(2) respectively. Here θ_{12} is the angle between the propagation directions of the μ^+ and B_s in the rest frame of the $\mu^+\mu^-$ – pair. The angel

θ_{34} is the angle between the propagation directions of e^+ and B_s in the rest frame of the e^+e^- pair.

The importance of the pole contribution becomes obvious when we analyze the double differential distribution $\frac{d^2\text{Br}(\bar{B}_s \rightarrow \mu^+\mu^-e^+e^-)}{dx_{12}dx_{34}}$, which is presented in Fig. 6. The Fig. 6 features the $\phi(1020)$ resonance in the x_{12} and x_{34} channels and the “tails” from J/ψ and $\psi(2S)$ resonances contributions.

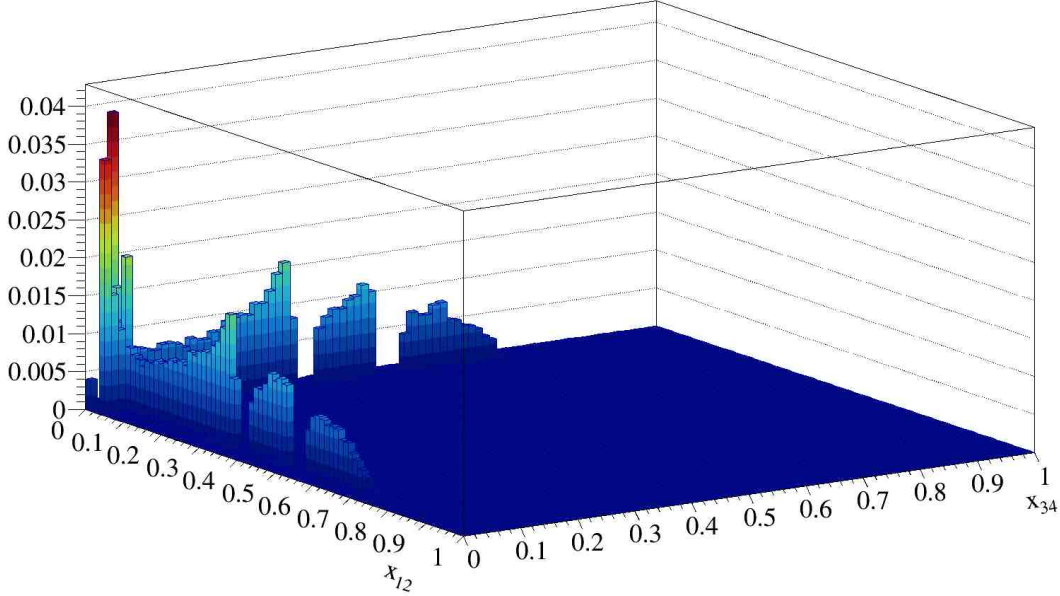


Figure 6. Double differential distribution $\frac{d^2\text{Br}(\bar{B}_s \rightarrow \mu^+\mu^-e^+e^-)}{dx_{12}dx_{34}}$

The forward – fackward lepton asymmetries are very sensitive to BSM physics. The asymmetry shape provides the fundamental information about the behaviour of the B_s amplitude and effects of intermediate resonances. For the decay $\bar{B}_s \rightarrow \mu^+\mu^-e^+e^-$ it is possible to forward – fackward lepton asymmetries $A_{FB}^{(\bar{B}_s)}(x_{12})$ and $A_{FB}^{(\bar{B}_s)}(x_{34})$ according to

$$A_{FB}^{(\bar{B}_s)}(x_{12}) = \frac{\int_0^1 dy_{12} \frac{d^2 \Gamma(\bar{B}_s \rightarrow \mu^+\mu^-e^+e^-)}{dx_{12} dy_{12}} - \int_{-1}^0 dy_{12} \frac{d^2 \Gamma(\bar{B}_s \rightarrow \mu^+\mu^-e^+e^-)}{dx_{12} dy_{12}}}{\frac{d \Gamma(\bar{B}_s \rightarrow \mu^+\mu^-e^+e^-)}{dx_{12}}}$$

and

$$A_{FB}^{(\bar{B}_s)}(x_{34}) = \frac{\int_0^1 dy_{34} \frac{d^2 \Gamma(\bar{B}_s \rightarrow \mu^+\mu^-e^+e^-)}{dx_{34} dy_{34}} - \int_{-1}^0 dy_{34} \frac{d^2 \Gamma(\bar{B}_s \rightarrow \mu^+\mu^-e^+e^-)}{dx_{34} dy_{34}}}{\frac{d \Gamma(\bar{B}_s \rightarrow \mu^+\mu^-e^+e^-)}{dx_{34}}}.$$

These asymmetries are shown in Fig. 7. The shape of asymmetries makes good sense in both channels and very similar to the shape of the asymmetries for the rare semileptonic decays of $B_{d,s}$ – mesons. It passes through zero in the region of small x_{12} (or x_{34}) and reflects the influence of the $\phi(1020)$. In the region of big x_{12} (or x_{34}) this shape demonstrates the relative signs between the higher excited charmonium states.

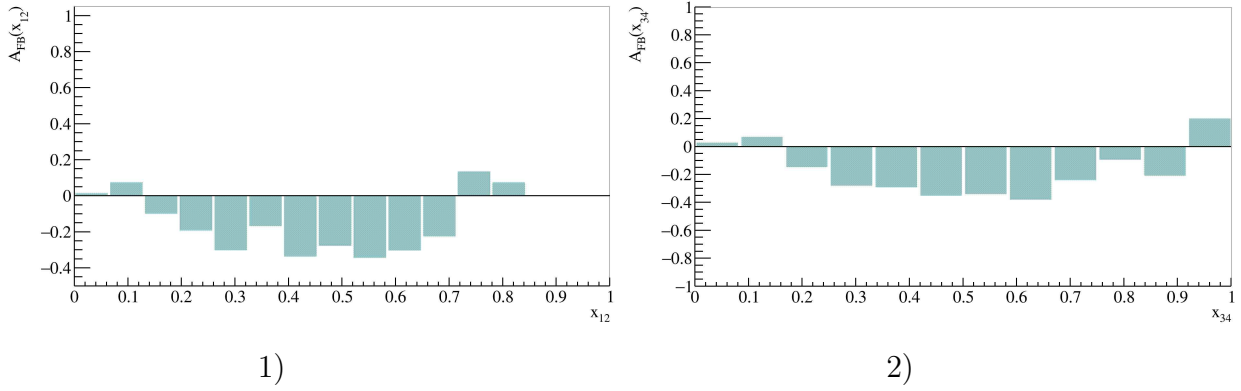


Figure 7. 1) The forward-backward leptonic asymmetry for the $\mu^+\mu^-$ - pair;
2) The forward-backward leptonic asymmetry for the e^+e^- - pair.

6. Conclusion

- In the framework of the Standard Model we present the predictions for the $\text{Br}(\bar{B}_s \rightarrow \mu^+\mu^-e^+e^-)$. We take into account resonant contributions $\phi(1020)$, $\psi(3770)$, $\psi(4040)$, $\psi(4160)$, $\psi(4415)$, $\rho(770)$ and $\omega(782)$. Also we consider “tails” contributions from J/ψ and $\psi(2S)$ resonances, non – resonant contribution from $b\bar{b}$ - pairs, the weak annihilation contribution and the bremsstrahlung. For the excluded J/ψ and $\psi(2S)$ resonances in accordance with [9, 10] we have

$$\text{Br}(\bar{B}_s \rightarrow \mu^+\mu^-e^+e^-) \approx (61 \pm 12) * 10^{-10};$$

If we exclude the contributions of $\phi(1020)$, J/ψ and $\psi(2S)$ in accordance with [16], we obtain

$$\text{Br}(\bar{B}_s \rightarrow \mu^+\mu^-e^+e^-) \approx (2.5 \pm 0.5) * 10^{-10};$$

- We provide the estimation for the branching ratio of $\bar{B}_s \rightarrow \mu^+\mu^-\mu^+\mu^-$ decay at the level

$$\text{Br}(\bar{B}_s \rightarrow \mu^+\mu^-\mu^+\mu^-) \sim 10^{-10}.$$

This prediction is consistent with the recent experimental upper limit from [16];

- Using the EvtGen-based generator model, we obtain the set of differential distributions for the $\bar{B}_s \rightarrow \mu^+\mu^-e^+e^-$ decay.

Acknowledgements

This paper is dedicated to the memory of Konstantin Toms, dear colleague and friend, who took interest in this work and did not live to see it published.

The authors would like to thank I. M. Belyaev (ITEP), E. E. Boos (SINP MSU), L. V. Dudko (SINP MSU), D. I. Melikhov (SINP MSU), V. Yu. Yegorychev (ITEP), and D. V. Savrina (ITEP, SINP MSU) for fruitful discussions which improved the current work significantly.

N. Nikitin was supported by RFBR under project 19-52-15022.

A. Danilina is grateful to the Basis Foundation for her stipend for Ph.D. students and express her gratitude to the Olga Igonkina Foundation for supporting this work.

Appendix A. Kinematics of four-lepton decays

Denote the four-momenta of the final leptons in four-leptonic decays of B -mesons as k_i , $i = \{1, 2, 3, 4\}$. Let

$$q = k_1 + k_2; \quad k = k_3 + k_4; \quad \tilde{q} = k_1 + k_4; \quad \tilde{k} = k_2 + k_3; \quad p = k_1 + k_2 + k_3 + k_4,$$

where p is the four-momentum of the B -meson and $p^2 = M_1^2$. For the calculations below it is suitable to use the dimensionless variables:

$$x_{12} = \frac{q^2}{M_1^2}, \quad x_{34} = \frac{k^2}{M_1^2}, \quad x_{14} = \frac{\tilde{q}^2}{M_1^2}, \quad x_{23} = \frac{\tilde{k}^2}{M_1^2}.$$

By common notation, $x_{ij} = (k_i + k_j)^2/M_1^2$. Hence $x_{ij} = x_{ji}$. The leptons may be considered as massless in almost all of the calculations of the present work, i.e., $k_i^2 = 0$. However during the calculation of the bremsstrahlung contribution in the area q^2 and k^2 , it is necessary to take into account the dependence of the bremsstrahlung matrix element and phase space on values of m_e and m_μ .

Let us find the intervals for x_{ij} using the inequality $(p_1 p_2) \geq \sqrt{p_1^2 p_2^2}$; then any $x_{ij} \geq (\hat{m}_i + \hat{m}_j)^2$. On the other hand,

$$1 = \frac{p^2}{M_1^2} = \frac{(q + k)^2}{M_1^2} \geq \frac{(\sqrt{q^2} + \sqrt{k^2})^2}{M_1^2} = \left(\sqrt{x_{12}} + \sqrt{x_{34}} \right)^2.$$

As $(\hat{m}_3 + \hat{m}_4)^2 \leq x_{34}$, then $x_{12} \leq 1$, so $x_{12} \in [0, 1]$. The upper limit of the variable x_{34} depends on the value of x_{12} :

$$x_{34} = \frac{(p - q)^2}{M_1^2} \leq \frac{(M_1 - \sqrt{q^2})^2}{M_1^2} = (1 - \sqrt{x_{12}})^2.$$

Thus for a fixed value of x_{12} the variable $x_{34} \in \left[(\hat{m}_3 + \hat{m}_4)^2, (1 - \sqrt{x_{12}})^2 \right]$.

Consider the kinematics of the decay $\bar{B}_s(p) \rightarrow \mu^+(k_1) \mu^-(k_2) e^+(k_3) e^-(k_4)$. We define an angle θ_{12} between the momentum of μ^+ and the direction of the \bar{B}_s -meson (z -axis) in the rest frame of the $\mu^+ \mu^-$ pair, and another angle θ_{34} between the direction

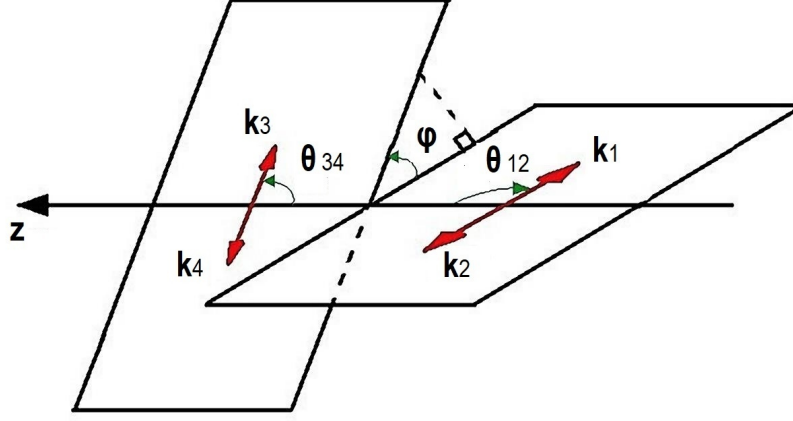


Figure A1. Kinematics of the decay $\bar{B}_s(p) \rightarrow \mu^+(k_1) \mu^-(k_2) e^+(k_3) e^-(k_4)$. Angle θ_{12} is defined in the rest frame of $\mu^+ \mu^-$ -pair; angle θ_{34} is defined in the rest frame of $e^+ e^-$ -pair; angle φ is defined in the rest frame of \bar{B}_s -meson.

of the e^+ and the direction of the \bar{B}_s - meson (z -axis) in the rest frame of $e^+ e^-$ - pair. Then

$$\begin{aligned} y_{12} &\equiv \cos \theta_{12} = \frac{1}{\lambda^{1/2}(1, x_{12}, x_{34})} (x_{23} + x_{24} - x_{13} - x_{14}), \\ y_{34} &\equiv \cos \theta_{34} = \frac{1}{\lambda^{1/2}(1, x_{12}, x_{34})} (x_{14} + x_{24} - x_{13} - x_{23}), \end{aligned} \quad (\text{A.1})$$

where $\lambda(a, b, c) = a^2 + b^2 + c^2 - 2ab - 2ac - 2bc$, the triangle function. Angles $\theta_{12} \in [0, \pi]$ and $\theta_{34} \in [0, \pi]$. Hence $y_{12} \in [-1, 1]$ and $y_{34} \in [-1, 1]$. Angles are measured relative to z -axis. Also let us define an angle $\varphi \in [0, 2\pi)$ in the rest frame of the \bar{B}_s -meson between the planes which are set by the pairs of vectors $(\mathbf{k}_1, \mathbf{k}_2)$ and $(\mathbf{k}_3, \mathbf{k}_4)$. Introduce a vector $\mathbf{a}_1 = \mathbf{k}_1 \times \mathbf{k}_2$, perpendicular to the plane $(\mathbf{k}_1, \mathbf{k}_2)$, and vector $\mathbf{a}_3 = \mathbf{k}_4 \times \mathbf{k}_3$, which are normal to the plane $(\mathbf{k}_3, \mathbf{k}_4)$. Then

$$\cos \varphi = \frac{(\mathbf{a}_1, \mathbf{a}_3)}{|\mathbf{a}_1| |\mathbf{a}_3|}.$$

It is suitable to choose $x_{12}, x_{34}, y_{12}, y_{34}$, and φ as independent integration variables. Then the four body phase space has the form

$$d\Phi_4 = \frac{M_1^4}{2^{14} \pi^6} \lambda^{1/2}(1, x_{12}, x_{34}) \sqrt{1 - \frac{4\hat{m}_\mu^2}{x_{12}}} \sqrt{1 - \frac{4\hat{m}_e^2}{x_{34}}} dx_{12} dx_{34} dy_{12} dy_{34} d\varphi, \quad (\text{A.2})$$

where $\hat{m}_\mu = m_\mu/M_1$ and $\hat{m}_e = m_e/M_1$.

This paper use notations almost identical to the notations of Ref. [20], except for y_{ij} , which here have the opposite sign compared to Ref. [20].

Appendix B. Dimensionless non – zero functions $a^{(ij)}$, $b^{(ij)}$, $c^{(ij)}$, $d^{(ij)}$, $f^{(ij)}$ and $g^{(ij)}$

Here we define the dimensionless functions from the (4) decay amplitude.

$$a^{(VV)}(x_{12}, x_{34}) = \frac{1}{M_1^2} \left[\frac{4 \hat{m}_b C_{7\gamma}(\mu)}{x_{12}, x_{34}} \left(\frac{1}{2} (F_{TV}(q^2, k^2) + F_{TV}(k^2, q^2)) - \right. \right. \\ \left. \left. - \frac{\hat{M}_2 \hat{f}_\phi^{em}}{x_{34} - \hat{M}_2^2 + i\hat{\Gamma}_2 \hat{M}_2} T_1(q^2) - \frac{\hat{M}_2 \hat{f}_\phi^{em}}{x_{12} - \hat{M}_2^2 + i\hat{\Gamma}_2 \hat{M}_2} T_1(k^2) \right) + \right. \\ \left. + \frac{C_{9V}(q^2, \mu)}{x_{34}} \left(F_V(q^2, k^2) - \frac{2\hat{M}_2}{1 + \hat{M}_2} \frac{V(q^2) \hat{f}_\phi^{em}}{x_{34} - \hat{M}_2^2 + i\hat{\Gamma}_2 \hat{M}_2} \right) + \right. \\ \left. + \frac{C_{9V}(k^2, \mu)}{x_{12}} \left(F_V(k^2, q^2) - \frac{2\hat{M}_2}{1 + \hat{M}_2} \frac{V(k^2) \hat{f}_\phi^{em}}{x_{12} - \hat{M}_2^2 + i\hat{\Gamma}_2 \hat{M}_2} \right) \right];$$

$$a^{(VA)}(x_{12}, x_{34}) = \frac{1}{M_1^2} \frac{C_{10A}}{x_{12}} \left[F_V(k^2, q^2) - \frac{2\hat{M}_2}{1 + \hat{M}_2} \frac{V(k^2) \hat{f}_\phi^{em}}{x_{12} - \hat{M}_2^2 + i\hat{\Gamma}_2 \hat{M}_2} \right];$$

$$a^{(AV)}(x_{12}, x_{34}) = \frac{1}{M_1^2} \frac{C_{10A}}{x_{34}} \left[F_V(q^2, k^2) - \frac{2\hat{M}_2}{1 + \hat{M}_2} \frac{V(q^2) \hat{f}_\phi^{em}}{x_{34} - \hat{M}_2^2 + i\hat{\Gamma}_2 \hat{M}_2} \right];$$

$$b^{(VV)}(x_{12}, x_{34}) = \frac{1}{M_1^2} \left[\frac{2 \hat{m}_b C_{7\gamma}(\mu)}{x_{12}, x_{34}} \left(\frac{1 - x_{12} - x_{34}}{2} (F_{TA}(q^2, k^2) + F_{TA}(k^2, q^2)) - \right. \right. \\ \left. \left. - \frac{\hat{M}_2 (1 - \hat{M}_2^2) \hat{f}_\phi^{em}}{x_{34} - \hat{M}_2^2 + i\hat{\Gamma}_2 \hat{M}_2} T_2(q^2) - \frac{\hat{M}_2 (1 - \hat{M}_2^2) \hat{f}_\phi^{em}}{x_{12} - \hat{M}_2^2 + i\hat{\Gamma}_2 \hat{M}_2} T_2(k^2) \right) + \right. \\ \left. + \frac{C_{9V}(q^2, \mu)}{x_{34}} \left(\frac{1}{2} (1 - x_{12} - x_{34}) F_A(q^2, k^2) - \frac{\hat{M}_2 (1 + \hat{M}_2) \hat{f}_\phi^{em}}{x_{34} - \hat{M}_2^2 + i\hat{\Gamma}_2 \hat{M}_2} A_1(q^2) \right) + \right. \\ \left. + \frac{C_{9V}(k^2, \mu)}{x_{12}} \left(\frac{1}{2} (1 - x_{12} - x_{34}) F_A(k^2, q^2) - \frac{\hat{M}_2 (1 + \hat{M}_2) \hat{f}_\phi^{em}}{x_{12} - \hat{M}_2^2 + i\hat{\Gamma}_2 \hat{M}_2} A_1(k^2) \right) \right];$$

$$b^{(VA)}(x_{12}, x_{34}) = \frac{1}{M_1^2} \frac{C_{10A}(\mu)}{x_{12}} \left[\frac{1 - x_{12} - x_{34}}{2} F_A(k^2, q^2) - \frac{\hat{M}_2 (1 + \hat{M}_2) \hat{f}_\phi^{em}}{x_{12} - \hat{M}_2^2 + i\hat{\Gamma}_2 \hat{M}_2} A_1(k^2) \right];$$

$$b^{(AV)}(x_{12}, x_{34}) = \frac{1}{M_1^2} \frac{C_{10A}(\mu)}{x_{34}} \left[\frac{1 - x_{12} - x_{34}}{2} F_A(q^2, k^2) - \frac{\hat{M}_2 (1 + \hat{M}_2) \hat{f}_\phi^{em}}{x_{34} - \hat{M}_2^2 + i\hat{\Gamma}_2 \hat{M}_2} A_1(q^2) \right];$$

$$\begin{aligned}
c^{(VV)}(x_{12}, x_{34}) = & \frac{1}{M_1^2} \left[\frac{2\hat{m}_b C_{7\gamma}(\mu)}{x_{12}, x_{34}} \left(\frac{1}{2} (F_{TA}(q^2, k^2) + F_{TA}(k^2, q^2)) - \right. \right. \\
& - \frac{\hat{M}_2 \hat{f}_\phi^{em}}{x_{34} - \hat{M}_2^2 + i\hat{\Gamma}_2 \hat{M}_2} \left(T_2(q^2) + \frac{T_3(q^2) x_{12}}{(1 - \hat{M}_2^2)} \right) - \\
& - \frac{\hat{M}_2 \hat{f}_\phi^{em}}{x_{12} - \hat{M}_2^2 + i\hat{\Gamma}_2 \hat{M}_2} \left(T_2(k^2) + \frac{T_3(k^2) x_{34}}{(1 - \hat{M}_2^2)} \right) \Bigg) + \\
& + \frac{C_{9V}(q^2, \mu)}{x_{34}} \left(\frac{1}{2} F_A(q^2, k^2) - \frac{\hat{M}_2}{(1 + \hat{M}_2)} \frac{A_2(q^2) \hat{f}_\phi^{em}}{x_{34} - \hat{M}_2^2 + i\hat{\Gamma}_2 \hat{M}_2} \right) + \\
& + \frac{C_{9V}(k^2, \mu)}{x_{12}} \left(\frac{1}{2} F_A(k^2, q^2) - \frac{\hat{M}_2}{(1 + \hat{M}_2)} \frac{A_2(k^2) \hat{f}_\phi^{em}}{x_{12} - \hat{M}_2^2 + i\hat{\Gamma}_2 \hat{M}_2} \right) \Bigg];
\end{aligned}$$

$$c^{(VA)}(x_{12}, x_{34}) = \frac{1}{M_1^2} \frac{C_{10A}(\mu)}{x_{12}} \left[\frac{1}{2} F_A(k^2, q^2) - \frac{\hat{M}_2}{1 + \hat{M}_2} \frac{A_2(k^2) \hat{f}_\phi^{em}}{x_{12} - \hat{M}_2^2 + i\hat{\Gamma}_2 \hat{M}_2} \right];$$

$$c^{(AV)}(x_{12}, x_{34}) = \frac{1}{M_1^2} \frac{C_{10A}(\mu)}{x_{34}} \left[\frac{1}{2} F_A(q^2, k^2) - \frac{\hat{M}_2}{1 + \hat{M}_2} \frac{A_2(q^2) \hat{f}_\phi^{em}}{x_{34} - \hat{M}_2^2 + i\hat{\Gamma}_2 \hat{M}_2} \right];$$

$$d^{(AV)}(x_{12}, x_{34}) = \frac{1}{M_1^2} \frac{C_{10A}(\mu)}{x_{34}} \frac{\hat{f}_\phi^{em}}{x_{34} - \hat{M}_2^2 + i\hat{\Gamma}_2 \hat{M}_2} \left[\frac{A_2(q^2)}{1 + \hat{M}_2} + \frac{2\hat{M}_2}{x_{12}} \left(A_3(q^2) - A_0(q^2) \right) \right];$$

$$g^{(VA)}(x_{12}, x_{34}) = \frac{1}{M_1^2} \frac{C_{10A}(\mu)}{x_{12}} \frac{\hat{f}_\phi^{em}}{x_{12} - \hat{M}_2^2 + i\hat{\Gamma}_2 \hat{M}_2} \left[\frac{A_2(k^2)}{1 + \hat{M}_2} + \frac{2\hat{M}_2}{x_{34}} \left(A_3(k^2) - A_0(k^2) \right) \right];$$

The dimensionless functions for the bremsstrahlung amplitude (Eq. 5):

$$d^{(VP)}(x_{12}, x_{123}, x_{124}) = - \frac{4C_{10A} \hat{m}_e \hat{f}_{B_s}}{M_1^2} \frac{1}{x_{12} (x_{124} - \hat{m}_e^2) (x_{123} - \hat{m}_e^2)} \frac{(k_3 - k_4, q)}{M_1^2},$$

$$f^{(VT)}(x_{12}, x_{123}, x_{124}) = - \frac{2C_{10A} \hat{m}_e \hat{f}_{B_s}}{M_1^2} \frac{1}{x_{12} (x_{124} - \hat{m}_e^2) (x_{123} - \hat{m}_e^2)} \frac{1 + x_{12} - x_{34}}{2}.$$

These are d – and f – functions for the $\mu^+ \mu^-$ – pair emitted by electron and positron in the final state (see first two diagrams on Fig. 3). For the $e^+ e^-$ – pair emitted by μ^+ and μ^- functions are similar.

In all formulae we use dimensionless variables $x_{12} = q^2/M_1^2$, and $x_{34} = k^2/M_1^2$, $\hat{f}_\phi^{em} = f_\phi^{em}/M_1$, $\hat{M}_2 = M_2/M_1$, and $\hat{\Gamma}_2 = \Gamma_2/M_1$. Form factors $F_{TV}(q^2)$, $T_1(q^2)$, $F_V(q^2, k^2)$, $V(q^2)$, $F_{TA}(q^2, k^2)$, $T_2(q^2)$, $F_A(q^2, k^2)$, $A_1(q^2)$ and $A_2(k^2)$ are also dimensionless functions [18].

- [1] M. D. Mauro, M. W. Winkler, "Characteristics of the Galactic Center excess measured with 11 years of Fermi-LAT data", Phys. Rev. D 103, 123005, 2021.
- [2] B. Abi et al. [Muon g-2 Collaboration], "Measurement of the Positive Muon Anomalous Magnetic Moment to 0.46 ppm", Phys. Rev. Lett. 126, 141801, 2021.
- [3] V. Khachatryan *et al.* [CMS and LHCb Collaborations], "Observation of the rare $B_s^0 \rightarrow \mu^+ \mu^-$ decay from the combined analysis of CMS and LHCb data", Nature 522, 68, 2015.
- [4] M. Aaboud *et al.* [ATLAS Collaboration], "Study of the rare decays of B_s^0 and B^0 into muon pairs from data collected during the LHC Run 1 with the ATLAS detector", Eur. Phys. J. C 76, no. 9, 513, 2016.
- [5] R. Aaij *et al.* [LHCb Collaboration], "Measurement of the $B_s^0 \rightarrow \mu^+ \mu^-$ branching fraction and effective lifetime and search for $B^0 \rightarrow \mu^+ \mu^-$ decays", Phys. Rev. Lett. 118, no. 19, 191801, 2017.
- [6] R. Aaij *et al.* [LHCb Collaboration], "Measurement of the $B_s^0 \rightarrow \mu^+ \mu^-$ decay properties and search for the $B^0 \rightarrow \mu^+ \mu^-$ and $B_s^0 \rightarrow \mu^+ \mu^- \gamma$ decays", Submitted to Phys. Rev. D, 2021.
- [7] A. Datta, J. Kumar, D. London, "The B anomalies and new physics in $b \rightarrow e^+ e^-$ ", Phys. Rev. B 797, 134858, 2019.
- [8] Belle II experiment: status and prospects, <https://aip.scitation.org/doi/abs/10.1063/5.0008685>.
- [9] R. Aaij *et al.* [LHCb Collaboration], "Search for decays of neutral beauty mesons into four muons", JHEP 1703, 001, 2017.
- [10] R. Aaij *et al.* [LHCb Collaboration], "Search for rare $B_{(s)}^0 \rightarrow \mu^+ \mu^- \mu^+ \mu^-$ decays", Phys. Rev. Lett. 110, 211801, 2013.
- [11] R. Aaij *et al.* [LHCb Collaboration], "Search for the rare decay $B^+ \rightarrow \mu^+ \mu^- \mu^+ \nu_\mu$ ", Eur. Phys. J. C 79, no. 8, 675, 2019.
- [12] Y. Dincer and L. M. Sehgal, "Electroweak effects in the double Dalitz decay $B_s \rightarrow \ell^+ \ell^- \ell'^+ \ell'^-$ ", Phys. Lett. B 556, 169, 2003.
- [13] A. V. Danilina and N. V. Nikitin, "Four-Leptonic Decays of Charged and Neutral B Mesons within the Standard Model", Phys. Atom. Nucl. 81, no. 3, 347 (2018) [Yad. Fiz. 81, no. 3, 331 (2018)].
- [14] A. J. Buras, M. Munz "Effective Hamiltonian for $B \rightarrow \ell^+ \ell^- X(s)$ e+ e- beyond leading logarithms in the NDR and HV schemes", Phys. Rev. Lett. 52, 186-195, 1995.
- [15] The development page for the EvtGen project, <https://evtgen.hepforge.org/>
- [16] R. Aaij *et al.* [LHCb Collaboration], "Searches for rare B_s^0 and B^0 decays into four muons", arXiv:2111.11339.
- [17] D. Melikhov, N. Nikitin, S. Simula, "Rare exclusive semileptonic $b \rightarrow s$ transitions in the standard model", Phys. Rev. D 57, p.333, 1998.
- [18] A. Kozachuk, D. Melikhov, N. Nikitin, "Rare FCNC radiative leptonic $B_{d,s} \rightarrow \ell^+ \ell^- \gamma$ decays in the standard model", Phys. Rev. D 97, 053007, 2018.
- [19] D. Melikhov, N. Nikitin, "Rare radiative leptonic decays $B_{d,s} \rightarrow \ell^+ \ell^- \gamma$ ", Phys. Rev. D 70, 114028, 2004.
- [20] A. R. Barker, H. Huang, P. A. Toale and J. Engle, "Radiative corrections to double Dalitz decays: Effects on invariant mass distributions and angular correlations", Phys. Rev. D 67, 033008, 2003.